Supplementary Information

Nuclear receptors control pro-viral and antiviral metabolic responses to hepatitis C virus infection

Gahl Levy[1,2,11], Naomi Habib[1,2,3,11], Maria Angela Guzzardi[1,4,11], Daniel Kitsberg[1,2], David Bomze[1,2], Elishai Ezra[1,5], Basak E. Uygun[6], Korkut Uygun[6], Martin Trippler[7], Joerg F. Schlaak[7], Oren Shibolet[8], Ella H. Sklan[9], Merav Cohen[1,2], Joerg Timm[10], Nir Friedman[1,2], Yaakov Nahmias[#,1,2]

1. *Grass Center for Bioengineering, Benin School of Computer Science and Engineering, The Hebrew University of Jerusalem, Israel*
2. *Silberman Institute of Life Sciences, The Hebrew University of Jerusalem, Israel*
3. *Klarman Cell Observatory, Broad Institute of Harvard and MIT, Cambridge, MA*
4. *Institute of Clinical Physiology, National Research Council (CNR), Pisa, Italy*
5. *Faculty of Engineering, Jerusalem College of Technology, Israel*
6. *Center for Engineering in Medicine, Massachusetts General Hospital, USA*
7. *Department of Gastroenterology and Hepatology, University Hospital, University Duisburg-Essen, Essen, Germany*
8. *Liver Unit, Department of Gastroenterology, Tel-Aviv Medical Center, Israel*
9. *Department of Clinical Microbiology and Immunology, Sackler School of Medicine, Tel Aviv University, Israel.*
10. *Institute for Virology, University Düsseldorf, Medical Faculty, Düsseldorf, Germany*
11. *These authors contributed equally to this work*

Correspondence should be addressed to:
Dr. Yaakov Nahmias
Director, Grass Center for Bioengineering
The Hebrew University of Jerusalem
Email: ynahmias@cs.huji.ac.il

Supplementary Information

Supplementary Results

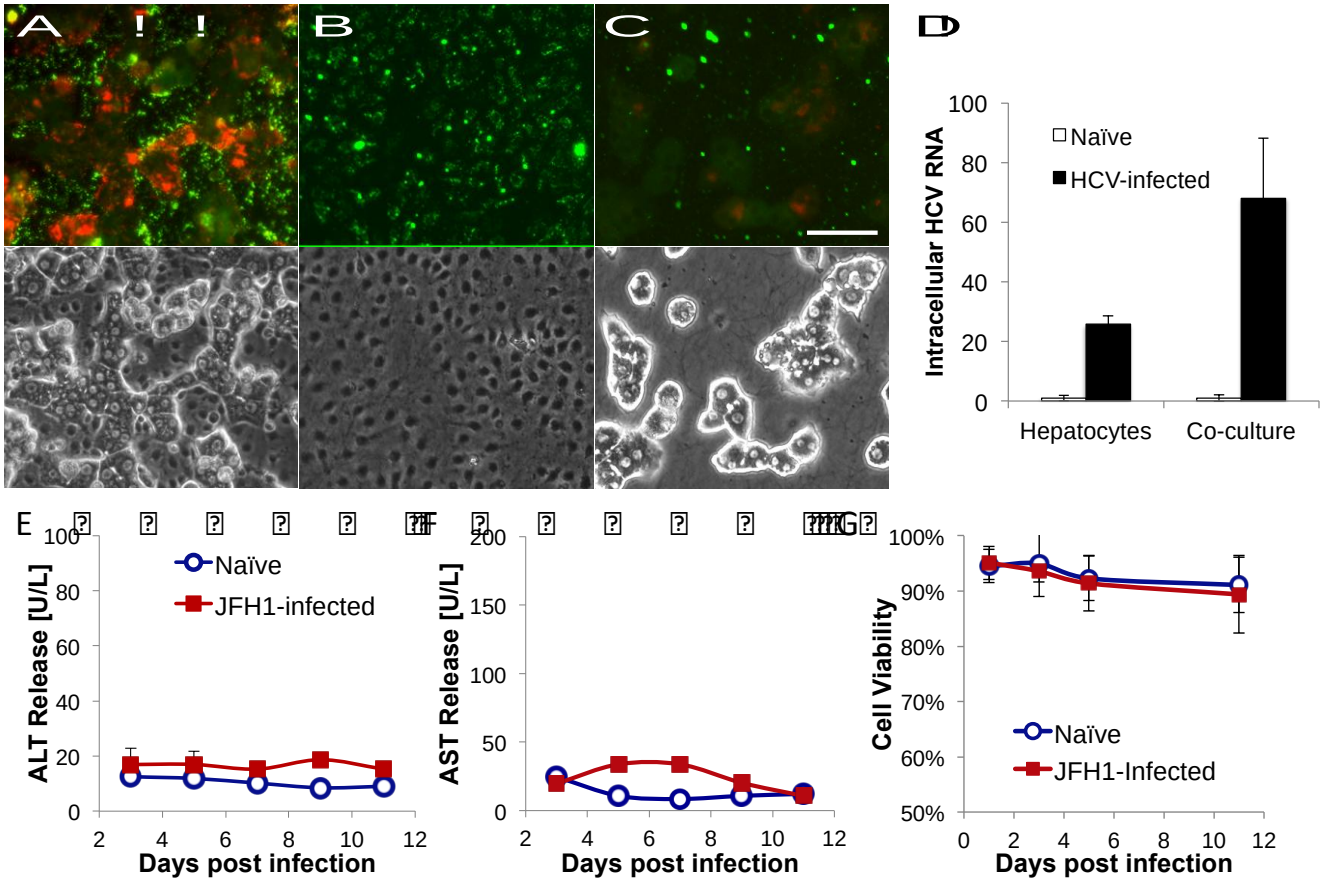

Supplementary Figure 1. Oxygenated cultures of primary hepatocytes and endothelial cells show higher susceptibility to HCV infection over monocultures while showing little loss of viability. Fluorescent and corresponding phase images of HCV pseudo particles (HCVpp) labeled green and DiI-LDL (*red*). A) Co-cultures of hepatocytes and endothelial cells show high level of LDL uptake by hepatocytes and binding of HCVpp by endothelial surface capture receptor L-SIGN. B) Monocultures of endothelial cells show HCVpp binding, but little LDL uptake. C) Monocultures of hepatocytes show very little HCVpp and LDL uptake. D) qRT-PCR at day 11 post-infection shows 3-fold higher levels of HCV RNA in co-cultures compared to primary hepatocyte alone ($p<0.001$, $n=3$). E) and F) Minimal release of liver enzymes alanine transaminase (ALT) aspartate transaminase (AST) demonstrates no significant loss of viability. G) Co-culture viability assessed by LIVE/DEAD staining was 90±5% for both conditions throughout the experiment.

Supplementary Information

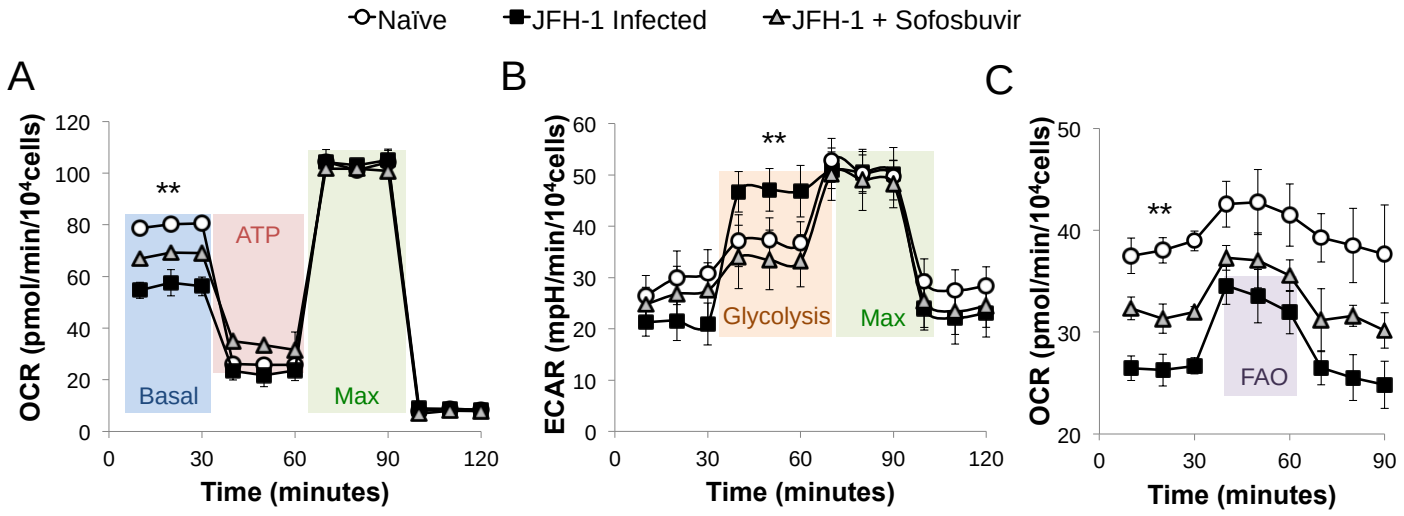

Supplementary Figure 2: Respiratory and glycolytic flux analysis of HCV-infected and sofosbuvir-treated primary human hepatocytes. A) Oxygen consumption rate (OCR) was measured on naïve and JFH-1 infected hepatocytes, as well as infected cells treated with HCV antiviral sofosbuvir (***methods***). Basal respiration (blue) was measured for 30 min showing significant differences between the three conditions ($p<0.001$, n=3). Oligomycin was injected at 30 min blocking ATP production due to oxidative phosphorylation (red). FCCP was injected at 60 min, followed by complex I and III inhibitors, injected at 90 min, showing no difference in maximum mitochondrial capacity for all conditions (green). B) Extra-cellular acidification rate (ECAR) was measured for 30 min in the absence of glucose providing baseline measurement. Rate of glycolysis was measured by injecting glucose at 30 min, followed by oligomycin-mediated inhibition of oxidative phosphorylation at 60 min. Finally, 2DG was injected at 90 min to block both pathways. The increase in ECAR due to the addition of glucose (orange) is defined as glycolysis rate, while the difference between oligomycin and 2DG treatments define the maximal glycolytic capacity of the cells (green). C) Rate of free fatty acid oxidation (FAO) was measured by injecting palmitate (C16:0) at 30 min, followed by complete inhibition of CPT-1 by etomoxir at 60 min. The difference in OCR between the treatments is defined as fatty acid oxidation rate (purple). ** $p < 0.001$; n = experimental replicates.

Supplementary Information

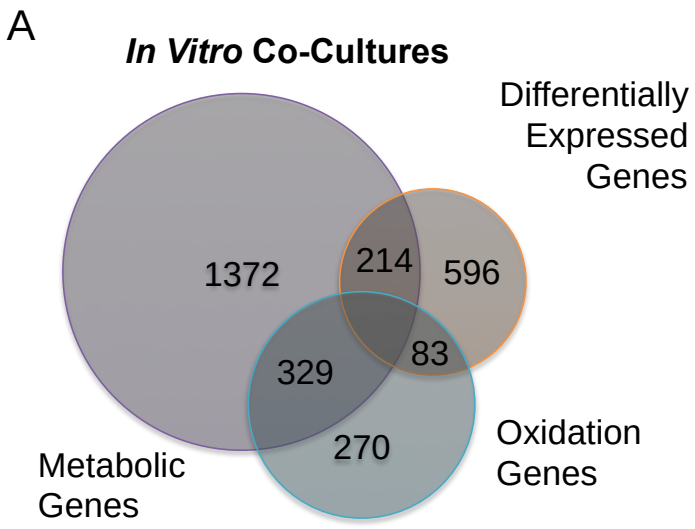

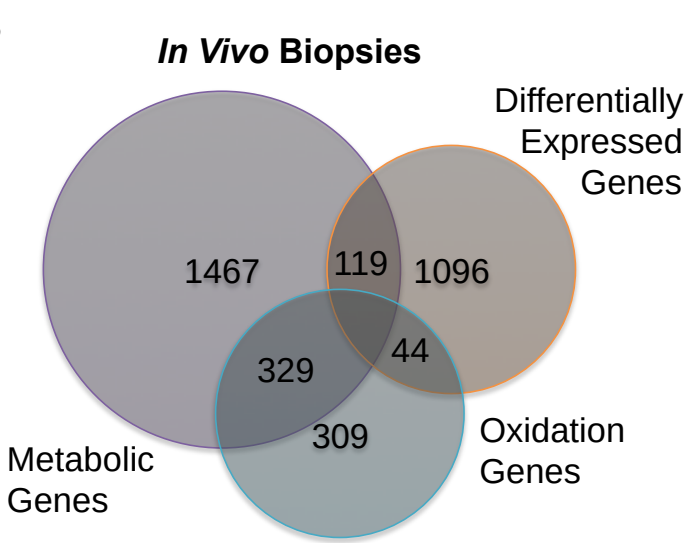

Unbiased Enrichment Analysis (In Vitro)

General Terms	Count	p-value	Bonferroni
GO:0042060~wound healing	43	1.98E-15	6.31E-12
GO:0009611~response to wounding	75	1.57E-14	4.94E-11
GO:0030198~extracellular matrix organization	29	5.24E-13	1.65E-09
GO:0009725~response to hormone stimulus	55	8.81E-12	2.78E-08
GO:0055114~oxidation reduction	78	1.02E-11	3.21E-08
GO:0016477~cell migration	42	2.27E-09	7.17E-06

Metabolism Terms	Count	p-value	Bonferroni
hsa00982:Drug metabolism	20	1.63E-08	2.84E-06
GO:0016053~organic acid biosynthesis	27	1.78E-07	5.62E-04
GO:0008202~steroid metabolic process	31	3.29E-07	1.04E-03
hsa00140:Steroid hormone biosynthesis	14	8.67E-06	1.51E-03
GO:0031667~response to nutrient levels	29	1.98E-06	6.24E-03
GO:0006638~neutral lipid metabolic process	13	9.07E-06	2.82E-02
hsa00500:Starch and sucrose metabolism	13	1.71E-05	2.97E-03

Enrichment of Defined Metabolic Categories	Count	Genes	Bonferroni
Drug Metabolism	22	69	1.13E-13
Cholesterol Metabolism	30	148	2.35E-12
Glucose Metabolism	65	506	1.22E-14
Lipid Metabolism	52	515	3.19E-08

Unbiased Enrichment Analysis (In Vivo)

General Terms	Count	p-value	Bonferroni
GO:0006955~immune response	87	1.54E-06	5.23E-03
GO:0019882~antigen processing and presentation	20	8.87E-06	2.98E-02
GO:0046649~lymphocyte activation	33	3.08E-05	9.96E-02
GO:0006968~cellular defense response	16	3.14E-05	1.02E-01
GO:0045321~leukocyte activation	37	5.60E-05	1.74E-01
GO:0008219~cell death	83	7.25E-05	2.19E-01

Metabolism Terms	Count	p-value	Bonferroni
None	-	-	-

Enrichment of Defined Metabolic Categories	Count	Genes	Bonferroni
Glucose Metabolism	86	732	1.22E-08
Nitrogen Metabolism	68	594	1.08E-06
Lipid Metabolism	66	764	5.09E-03

Supplementary Figure 3. Gene expression and enrichment analysis of HCV infection. A) Venn diagram of the 893 differentially regulated genes identified in JFH-1-infected co-cultures compared to controls. Close to 24% are related to metabolic function. Oxidative stress is another major category. Unbiased GO and Kegg enrichment analysis showed a complex response including wound healing ($p<10^{-11}$), oxidative stress ($p<10^{-7}$) drug and lipid metabolism ($p<1\times10^{-3}$). To focus on the transcriptional regulation of metabolism we grouped functional annotations into six metabolic categories (**Table 3**). The differentially expressed genes were significantly enriched in all categories, including: lipid metabolism ($p<10^{-7}$), cholesterol metabolism ($p<10^{-11}$), glucose metabolism ($p<10^{-13}$) and drug metabolism ($p<10^{-12}$). B) Venn diagram of the 1,259 differentially regulated genes identified in liver biopsies taken from HCV patients (low fibrosis) compared to biopsies of normal tissue. The differentially expressed genes identified *in vitro* were enriched with those found *in vivo* ($p<0.005$). Unbiased enrichment analysis showed a strong immune response, masking other effects. However, our defined categories included glucose ($p<10^{-7}$) and lipid metabolism ($p<0.01$) and were significantly enriched. Number of differentially expressed genes (count) and the total number of genes in the category (genes) are presented.

Supplementary Information

A

	Category Name	Size	NES	FDR q-val
Up	Drug Metabolism*	39	2.73	0.0001
	Fatty Acid Oxidation*	70	1.82	0.0065
	Bile Acid Biosynthesis*	24	1.77	0.0074
	Urea Cycle*	10	1.73	0.0068
	Glycolytic Process*	62	1.49	0.0498
	TCA Cycle	28	1.39	0.0833
	Gluconeogenesis	71	1.29	0.1421
	Fatty Acid Biosynthesis	113	1.27	0.1352
Down	Oxidative Phosphorylation	61	-0.42	0.9982

B

	Category Name	Size	NES	FDR q-val
Up	Drug Metabolism*	39	2.06	0.0001
	Fatty Acid Oxidation*	70	1.90	0.0024
	Oxidative Phosphorylation*	61	1.84	0.0028
	Bile Acid Biosynthesis*	24	1.75	0.0071
	Urea Cycle	10	1.36	0.1504
	Glycolytic Process	62	1.29	0.1982
	Fatty Acid Biosynthesis	113	1.20	0.2759
	Gluconeogenesis	71	1.19	0.2561
Down	TCA Cycle	28	0.89	0.6429

C

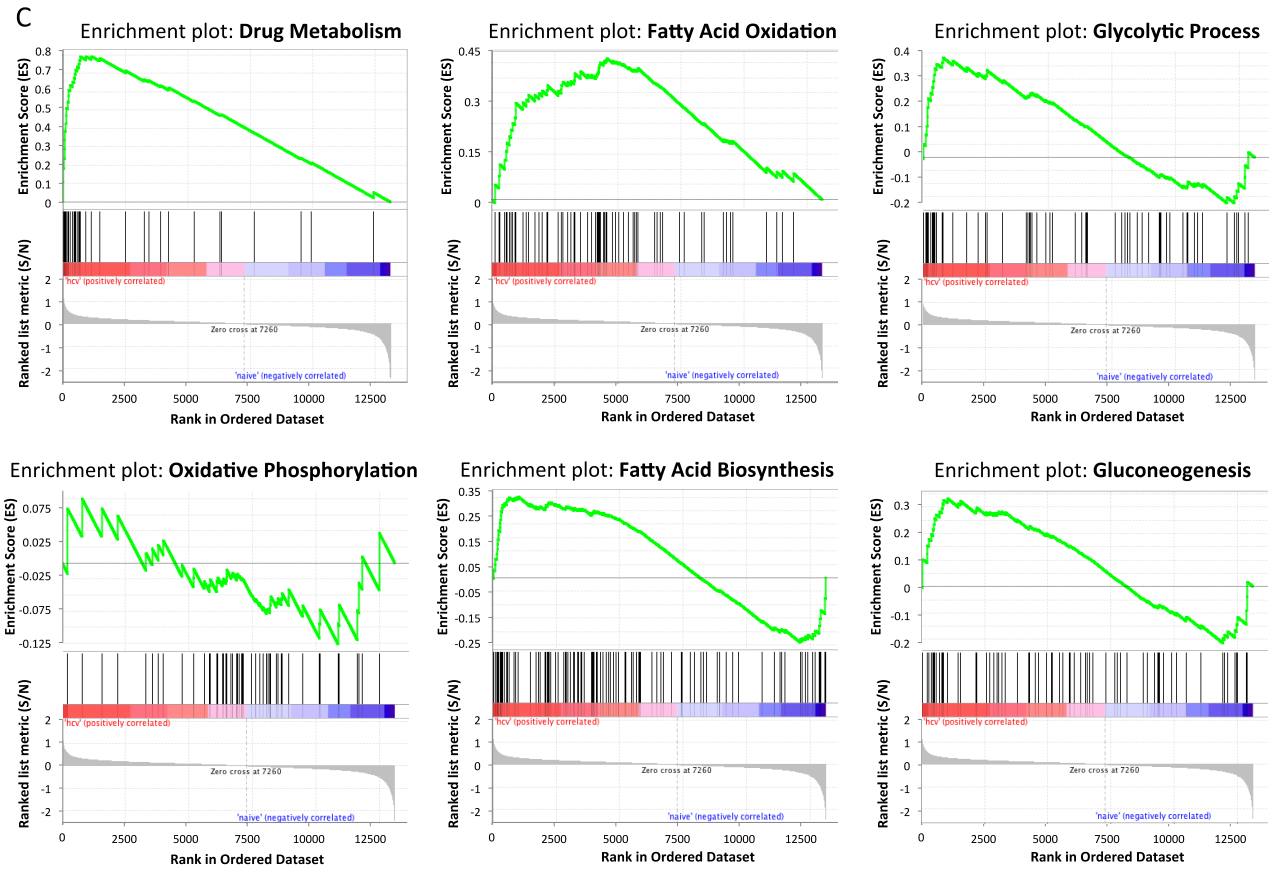

Supplementary Figure 4. Gene Set Enrichment Analysis (GSEA). A) GSEA on JFH-1 infected primary human hepatocyte co-cultures compared to naïve cells. Analysis show significant (*) HCV-induced up-regulation of drug metabolism ($p<0.0001$), fatty acid oxidation ($p<0.01$) and glycolytic process ($p<0.05$). Fatty acid biosynthesis and gluconeogenesis were induced but not significantly different from naïve cells. Oxidative phosphorylation was down-regulated by HCV-infection but was not significantly different from naïve cells. B) GSEA of HCV patients compared to normal human liver biopsy samples. Analysis show significant (*) HCV-induced up-regulation of drug metabolism ($p<0.0001$) and fatty acid oxidation ($p<0.01$), but no significant increase in glycolysis. Surprisingly, oxidative phosphorylation was significantly down-regulated by HCV-infection possibly due to the presence of multiple cell types in biopsy samples. C) GSEA enrichment plots showing *in vitro* effects of HCV infection (red/left) compared to naïve (blue/right).

Supplementary Information

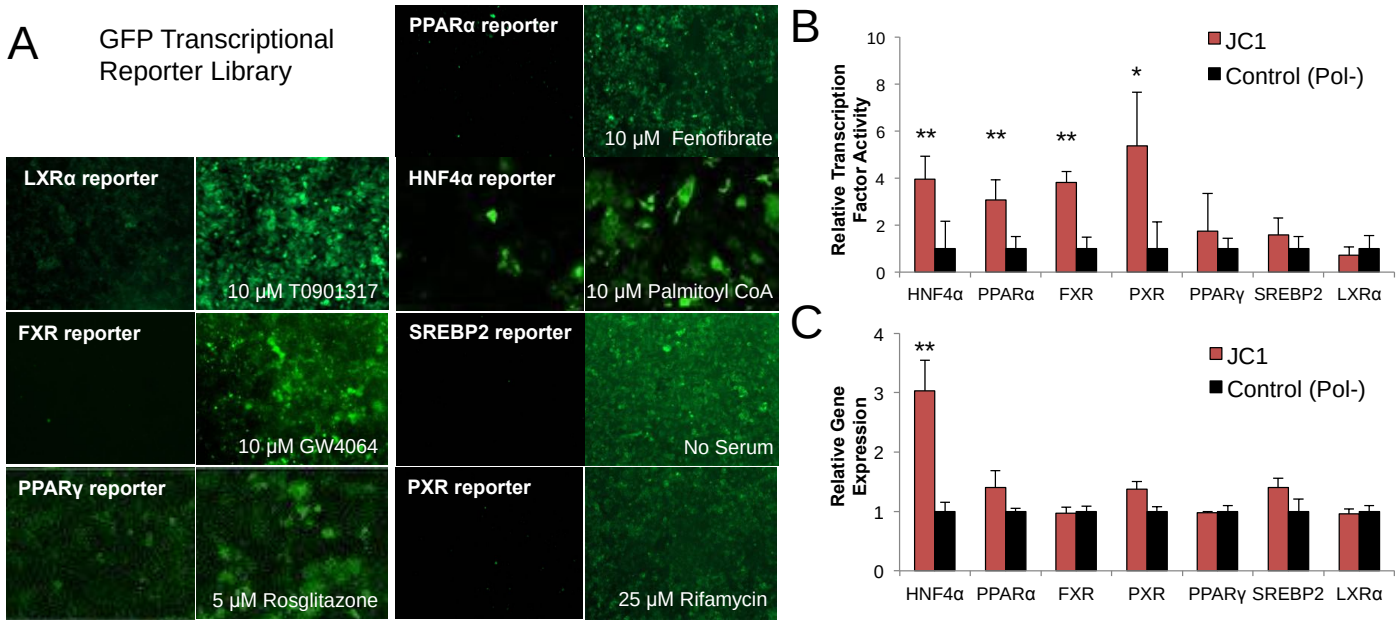

Supplementary Figure 5. Validation of GFP transcriptional activity reporter panel. A) Fluorescent micrographs of GFP transcriptional activity reporters for LXRα, FXR, PPARϒ, PPARα, HNF4α, SREBP2, and PXR. Reporters were generated by cloning multiple repeats of the transcription factor response element upstream of a minimal promoter (***methods***). Reporters were introduced into HepG2 or Huh7.5.1 cells using lentivirus infection and the cells were exposed to the classical agonist for 24 hours. B) Quantification of JC1/RFP induced activation of each GFP reporter (***methods***, **Fig. 3-5**). While HNF4α, PPARα, FXR and PXR showed significant elevation in activity following infection, we could not detect changes in the activity of PPARϒ, SREBP2, or LXRα. * $p<0.05$, ** $p<0.001$. C) qRT-PCR of the same transcription factors shows that only the expression of HNF4α changed ($p<0.001$, n=3), demonstrating the difficulties of discerning activity from gene expression data.

Supplementary Information

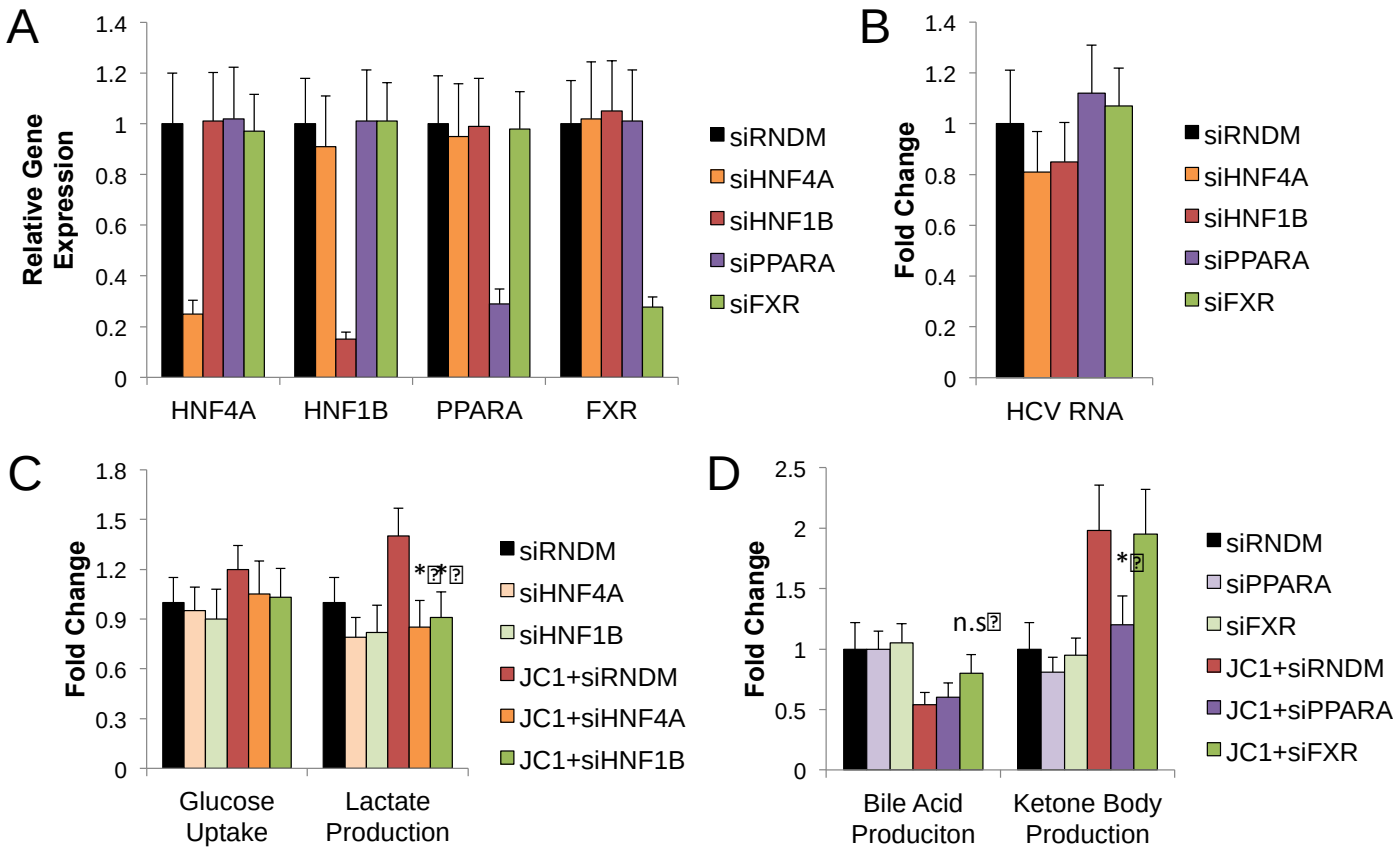

Supplementary Figure 6. Silencing RNAi screen against computationally identified HCV metabolic regulators. A) Gene expression analysis of transcription factor expression 72 hrs after liposome transfection with siRNA against HNF4α, HNF1β, PPARα, FXR and random RNA (RNDM) in Huh7.5.1 cells. Target gene expression was significantly reduced by 79-85% ($p<0.01$, n=3). B) Secreted HCV RNA was reduced by HNF4α and HNF1β inhibition by 19-15%, and increased by PPARα and FXR inhibition by 12-7%. C) Glucose uptake was induced by JC1 infection and reversed by HNF4α and HNF1β inhibition. Lactate production increased by 40±16% following JC1 infection ($p<0.05$, n=5) and was reversed by HNF4α and HNF1β inhibition ($p<0.05$, n=3). D) Bile acid production decreased by 46±10% following JC1 infection ($p<0.01$, n=5), remained unaffected by PPARα inhibition ($p<0.05$, n=3), but was partly reversed by FXR inhibition. Ketone body production increased by 2-folds following JC1 infection ($p<0.01$, n=5), remained unaffected by FXR inhibition, but was reversed by PPARα inhibition ($p<0.05$, n=3).

Supplementary Information

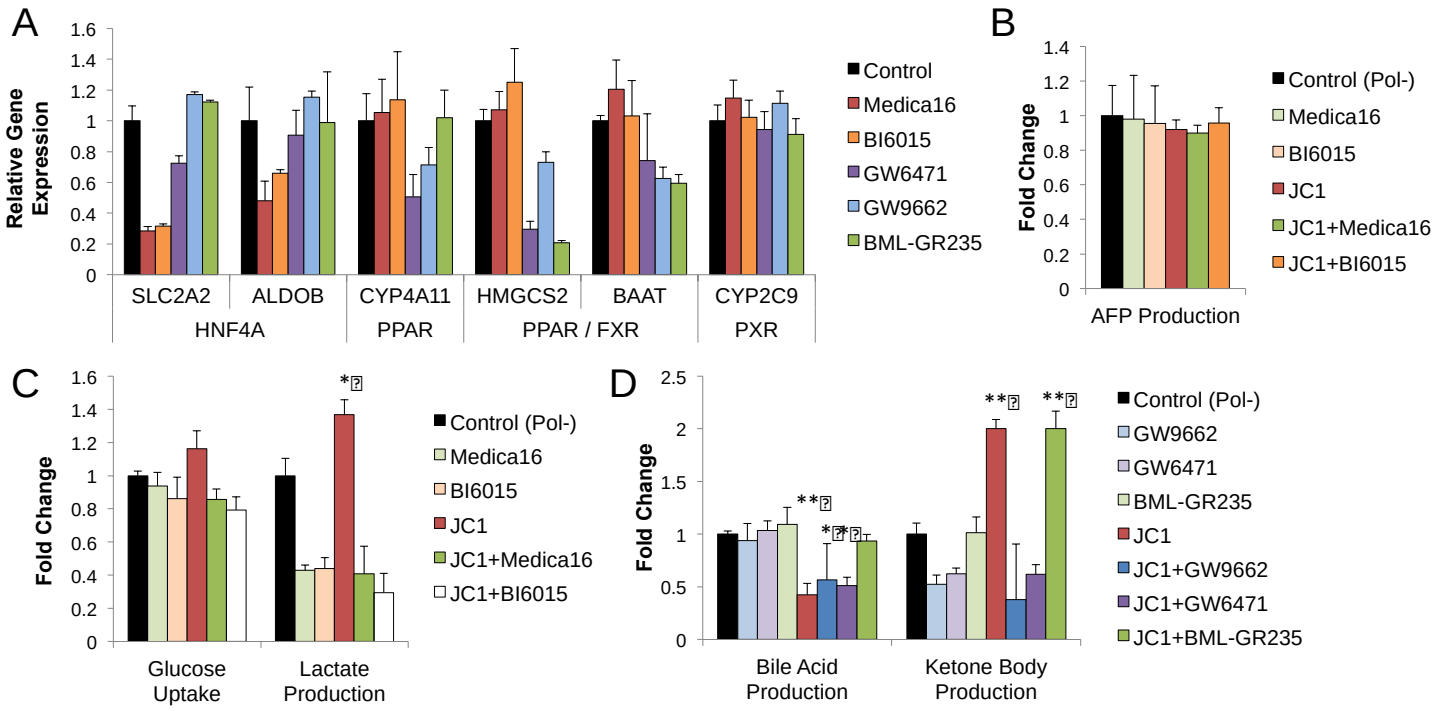

Supplementary Figure 7. Functional nuclear receptor perturbation using small molecule inhibitors shows nuclear receptor involvement in HCV metabolic regulation. A) Gene expression analysis of transcription factor inhibitor specificity in Huh7.5.1 cells exposed to the compounds for 24 hrs (***methods***). HNF4α inhibitors Medica16 and BI6015 show specific inhibition of target glycolysis genes SLC2A2 and ALDOB (**Fig. 3**). PPAR inhibitors GW6471 and GW9662 show inhibition of lipid metabolism genes CYP4A11, HMGCS2, and BAAT (**Fig. 4**), while BML-GR235 works on a subset related to cholesterol metabolism. Finally, the inhibitors do not affect PXR target gene CYP2C9. B) Analysis of alpha-fetoprotein (AFP) secretion comparing Medica16 and BI6015 treated JC1-infected and Pol$^-$ control cells show no effect of HNF4α inhibitors on liver function. C) Complete metabolic analysis of **Fig. 3F**, comparing Medica16 and BI6015 treated JC1-infected cells to similarly treated Pol$^-$ controls. Glucose uptake was induced by JC1 infection and reversed by treatment with HNF4α inhibitors Medica16 and BI6015, compared to similarly treated controls. Lactate production significantly increased by JC1 infection ($p<0.05$, $n=5$) and was reversed by treatment with Medica16 and BI6015, ($p<0.05$, $n=5$) compared to similarly treated controls. D) Complete metabolic analysis of **Fig. 4F**, comparing GW9662, GW6471 and BML-GR235 treated JC1-infected cells to similarly treated Pol$^-$ controls. Bile acid production was significantly reduced by JC1 infection ($p<0.01$, $n=5$) and unaffected by treatment with PPAR inhibitors GW9662 and GW6471 ($p<0.05$, $n=5$), but reversed by treatment with FXR inhibitor BML-GR235 ($p<0.05$, $n=5$). Ketone body production was significantly induced by JC1 infection ($p<0.01$, $n=5$) and unaffected by BML-GR235 treatment , but reversed by treatment with PPAR inhibitors GW9662 and GW6471 ($p<0.05$, $n=5$).

Supplementary Information

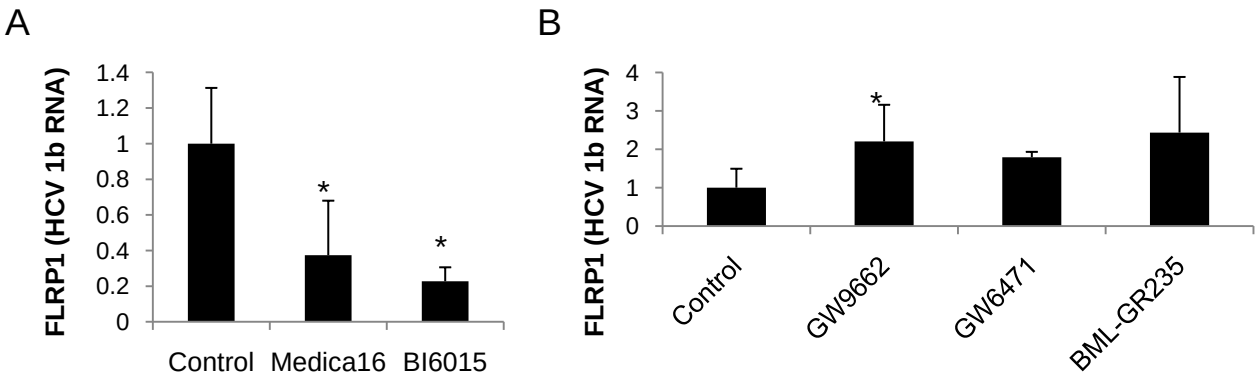

Supplementary Figure 8. Metabolic regulation of HCV genotype 1b in Huh7 cells. A) Huh7 cell line harboring a full-length genotype 1b replicon (Blight et al., 2000) was exposed to HNF4α inhibitors Medica16 and BI6015 for 24 hrs. qRT-PCR showed a significant 2- and 4-fold inhibition in HCV RNA following treatment, respectively. B) Genotype 1b cells were similarly exposed to PPAR inhibitors GW9662 and GW6471, as well as FXR inhibitor BML-GR235. qRT-PCR showed a 1.8 to 2.4-fold increase in HCV RNA following treatment. These results mirror our findings with JFH-1 and JC1 clones (genotype 2a).

Supplementary Information

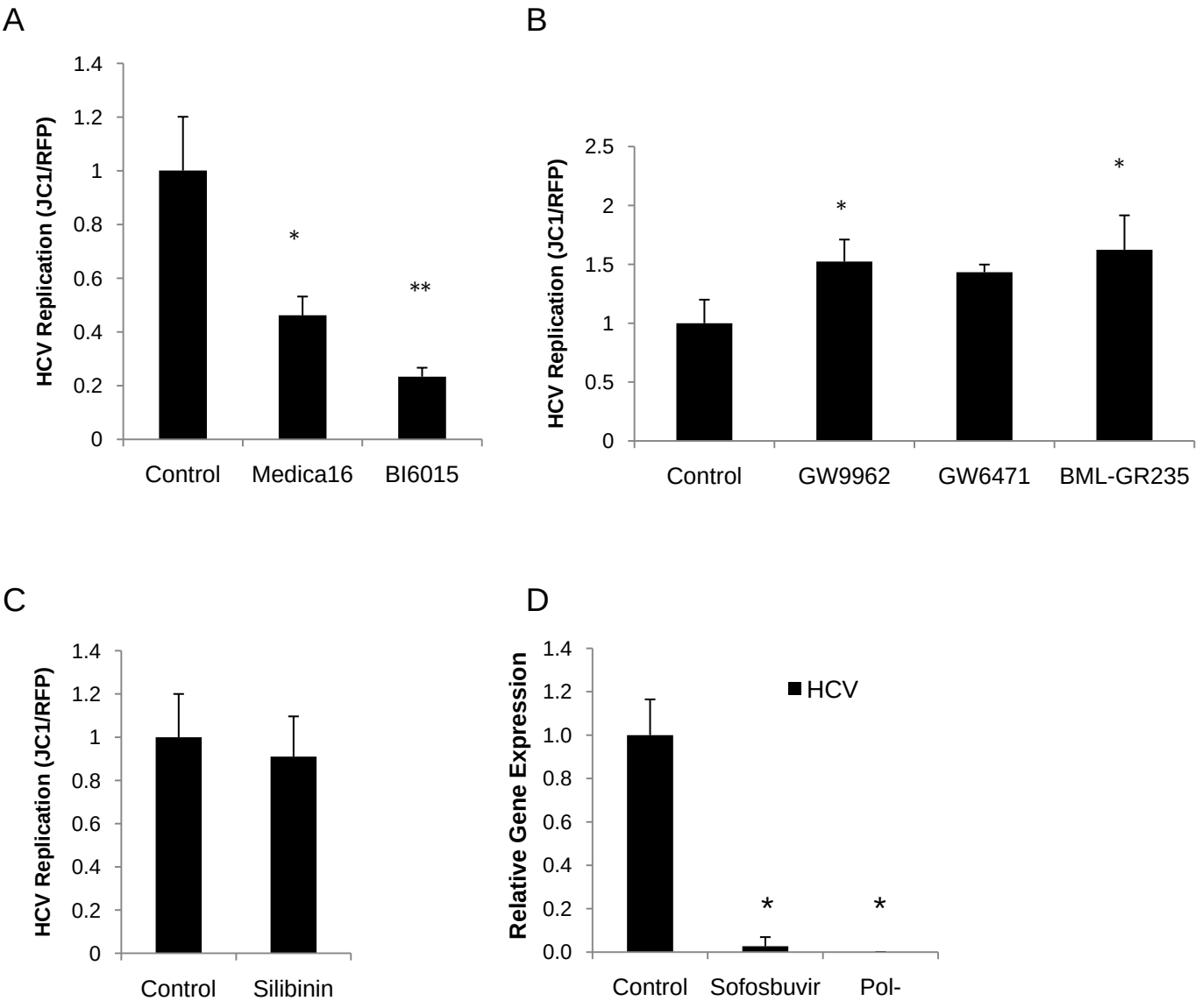

Supplementary Figure 9. Metabolic regulation of HCV in primary human hepatocytes. A) JC1/RFP infected primary human hepatocytes (***methods***) were exposed to HNF4α inhibitors Medica16 and BI6015 for 24 hrs. JC1/RFP showed a significant 2- and 4-fold inhibition in HCV replication ($p<0.05$ and $p<0.01$, n=4), respectively. B) Primary hepatocytes were similarly exposed to PPAR inhibitors GW9662 and GW6471, as well as FXR inhibitor BML-GR235. JC1/RFP showed a 1.4 to 1.6-fold increase in HCV replication following treatment. C) Primary hepatocytes exposed to PXR inhibitor silibinin showed no significant changes in HCV replication ($p=0.53$). These results mirror our findings with Huh7.5.1 cells. D) Gene expression analysis of HCV in JC1 infected primary human hepatocytes treated with sofosbuvir or vehicle control for 72 hrs. JC1 infected primary hepatocytes treated with sofosbuvir showed a 37-fold decrease in viral expression compared to untreated JC1 control ($p<0.05$ n=3), and was not significantly different than uninfected Pol^- cells ($p=0.17$, n=3). * $p<0.05$, ** $p<0.01$, n=experimental replicates

Supplementary Information

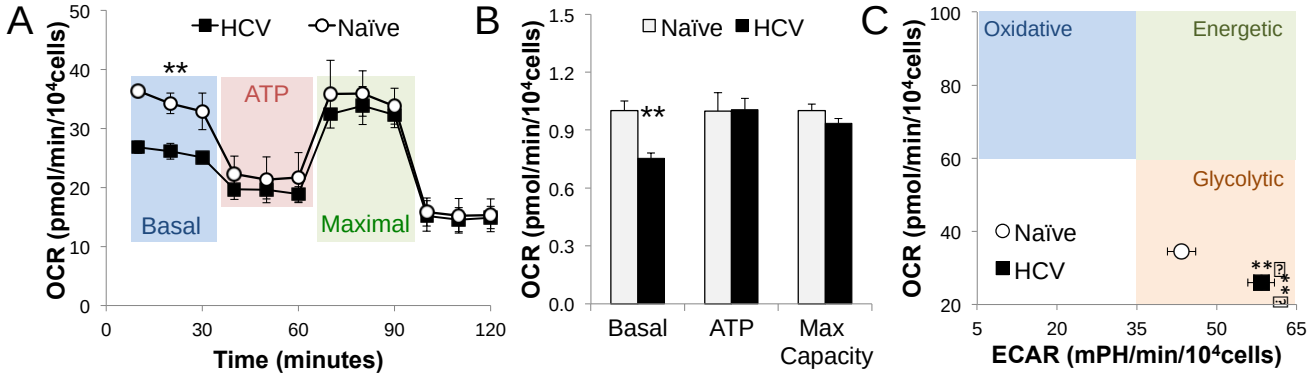

Supplementary Figure 10. Analysis of mitochondrial function in growth arrested Huh7.5 cells. Previous attempts to unravel the metabolic effects of viral infection relied on proliferating cancer cells, showing up-regulation of most metabolic pathways including glycolysis, oxidative phosphorylation and glutamine metabolism. In contrast, our metabolic analysis was carried out on non-proliferating primary human hepatocytes in which oxidative phosphorylation dominates over glycolysis and glutamine metabolism. We show a similar induction of glycolysis, but a critical down-regulation of oxidative phosphorylation and glutamine metabolism characteristic of the *Warburg effect.* Our analysis suggests that the cells circumvent mitochondrial pathways (**Fig. 1,2**). One reason for this discrepancy is that previous analysis utilized hepatoma cell lines whose proliferation rates may be affected by HCV infection. However, when Huh7.5 cells were growth arrested following culture in 1% DMSO, HCV infection caused a significant 11% reduction in basal mitochondrial activity ($p<0.05$ $n=6$), supporting our results. A) JC1/RFP infected (HCV) and naïve Huh7.5 cells were expanded in 1% DMSO for 6 days until cell proliferation ceased. Mitochondrial analysis was carried out on 10,000 cells in the Seahorse Bioscience XFp Flux analyzer. A time course for measurement of oxygen consumption rate (OCR) is shown under basal conditions, followed by the sequential addition of oligomycin (1 µM), FCCP (0.5 µM), and a mixture of antimycin A and rotenone (0.5 µM). B) Basal metabolic rate decreased in HCV-infected hepatocytes by 24% ($p<0.01$ $n=3$). C) Metabolic phenotype graph showing OCR and Extracellular acidification rate (ECAR), a measure of glycolysis, in naïve and JFH-1 infected Huh7.5.1 cells, showing the metabolic shift towards a more glycolytic phenotype.

Supplementary Information

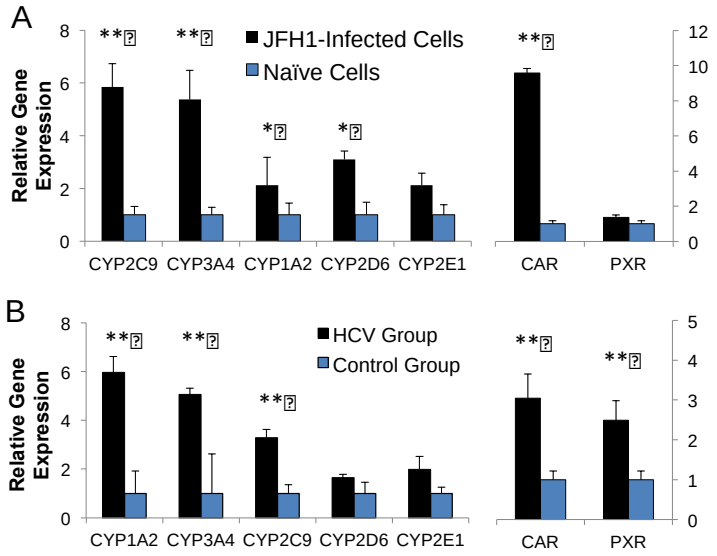

Supplementary Figure 11. HCV-induced CYP450 expression *in vitro* and *in vivo*. A) qRT-PCR analysis of CYP450 enzymes in JFH-1 infected co-cultures of primary human hepatocytes compared to mock-infected controls. PXR targets CYP3A4 and CYP2C9 show 5- and 6-fold induction, respectively. CYP1A2 and CYP2D6 show a milder, yet significant increase in expression. While PXR expression increased by 30%, CAR expression showed 9-fold induction. B) Analysis of CYP450 expression in liver biopsies obtained from HCV patients compared to normal livers. CYP3A4 and CYP2C9 show 5- and 3-fold induction, respectively. CYP1A2 shows a stronger 6-fold induction perhaps due to its presence in infiltrating immune cells. Expression levels of CAR and PXR show a 3 and 2-fold increase in expression, respectively.

Supplementary Information

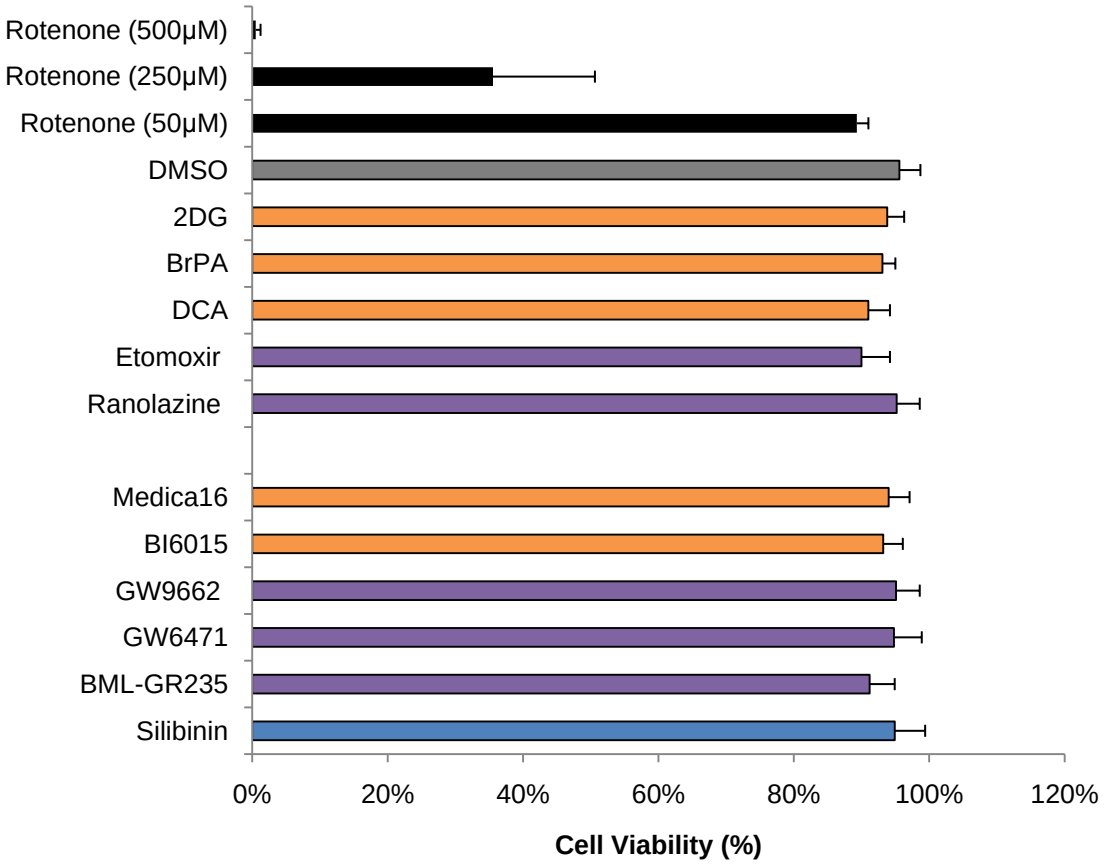

Supplementary Figure 12. **Inhibitor Cell Viability Analysis.** Small molecule inhibitors cause no toxicity in Huh7.5.1 cells following a 24-hour exposure based on fluorescent LIVE/DEAD viability analysis (***methods***). For glycolysis inhibitors, 2DG was used at 1 mM, BrPA at 10 μM, and DCA at 100 μM. For lipid metabolism inhibitors, etomoxir was used at 100 μM, and ranolazine at 50 μM. Nuclear receptor inhibitors (**Fig. 3-5**) Medica16 was used at 250 μM, BI6015 at 5 μM, GW9662 at 10 μM, GW6471 at 10 μM, BML-GR235 at 100 μM, and silibinin at 200 μM. Cell viability in all experimental conditions was greater than 90% and not significantly different from DMSO control. Rotenone, a mitochondrial complex I inhibitor, was used as positive control.

Supplementary Information

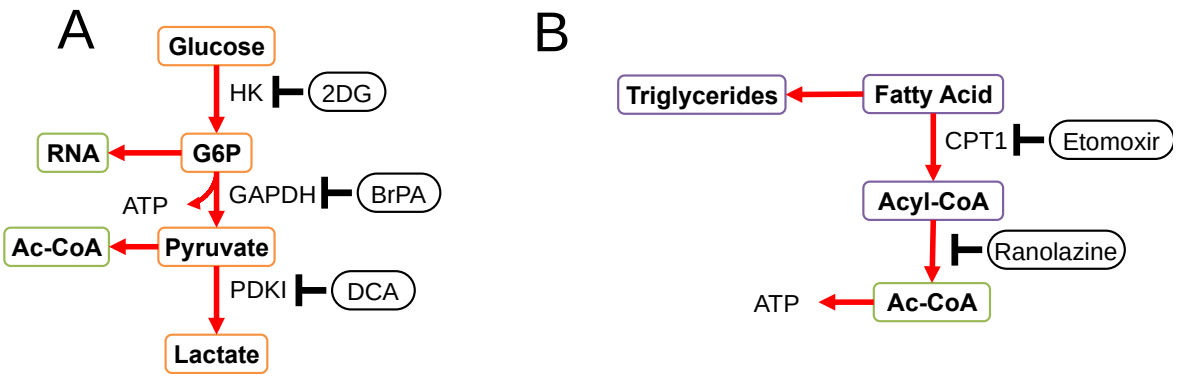

Supplementary Figure 13. Schematics of Metabolic Inhibitor Targets. A) Schematic of glycolysis with enzyme inhibitors 2DG, BrPA and DCA. B) Schematic of fatty acid oxidation and inhibitors etomoxir and ranolazine.

Supplementary Information

Supplementary Table 1. Metabolic flux analysis (MFA) model and quantitative results. Balance equations of the MFA model (fluxes 1-80) and quantitative results for HCV infected and mock-infected primary human hepatocytes.

Supplementary Table 2. Measured metabolic fluxes. Changes in external metabolites measured days 8 to 10 post-infection following metabolic stabilization for HCV infected and mock-infected primary human hepatocytes.

Supplementary Table 3. Defined metabolic categories for enrichment analysis. Collection of GO and KEGG categories used to define functional metabolic categories.

Supplementary Table 4. HCV activated transcriptional regulators by metabolic pathway (*in vitro*). Transcriptional regulatory analysis is used to identify transcription factors as activated if their target genes are enriched within the differentially expressed genes in each metabolic category. Transcription factors highlighted in green were evaluated using GFP activity reporter (***methods***).

Supplementary Table 5. HCV activated transcriptional regulators in general liver metabolism (*in vivo*). Transcriptional regulatory analysis is used to identify transcription factors as activated if their target genes are enriched within the differentially expressed genes in all metabolic categories combined (defined as general liver metabolism). Transcription factors highlighted in green were evaluated using GFP activity reporter (***methods***).

Nature Chemical Biology: doi:10.1038/nchembio.2193